https://doi.org/10.37434/tpwj2021.03.04

PECULIARITIES OF EMERGENCY FAILURE OF A PROCESS PIPELINE

M.D. Rabkina, V.A. Kostin and **T.G. Solomiichuk**
E.O. Paton Electric Welding Institute of the NAS of Ukraine
11 Kazymyr Malevych Str., 03150, Kyiv, Ukraine. E-mail: office@paton.kiev.ua

Analysis of failure of process pipeline, including a study of the properties, chemical composition and structure of the metal of welded joints, as well as the center of fracture and nature of crack propagation, made it possible to establish the most probable causes that led to its premature failure. It is assumed that such reasons are: a defect in a longitudinal weld; residual stresses in the pipe resulting from local heat treatment of the assembly circular weld; and probable longitudinal stresses arising from pipeline sagging between the supports. Ref. 9, 4 Tables, 7 Figures.

Keywords: technological pipeline; longitudinal and circumferential welded joints; defects in welded joints; lacks-of-fusion; structural heterogeneity; lamellar tearing; destruction

Pipeline failure, shutdown and accidents, as well as the extent and consequences of emergencies in gas and oil pipelines, both main and in-plant ones, largely depend on the quality and properties of pipe metal [1, 2]. During performance of complex pressure test of a technological pipeline (after operation for about 2.5 years on the whole) by technical nitrogen under pressure $P = 10^2$ MPa [3], its emergency depressurization took place. Data analysis suggested that the main factors, which could lead to pipeline destruction, alongside the possible nonconformity of the metal proper to the specified requirements, probably are: heat treatment of site circumferential welded joints (high-temperature tempering — heating up to the temperature of 760 ± 20 °C at three-hour soaking) that is conducted at welding of pipe sections; temperature mode of the process line, at which the pipe temperature in the destruction zone periodically varied from ambient temperature to 500 °C; and presence of bending stresses in the support zone.

Figure 1. Fragment of the dismantled pipe with fracture region and marks for cutting out templates for investigations and mechanical testing

Previous visual analysis of the destruction mode showed that fracture propagated both in base metal and in the HAZ, as well as in the circumferential site weld (Figure 1). Here, the failure center was not determined. Pipes were supplied for mounting in the form of sections from several shells after welding in the manufacturing plant. Then these sections were welded by site circumferential welds.

The objective of the studies was establishing the conformity of the initial material parameters to the specified (standard) values, detection of failure center, nature of crack propagation, as well as clarifying the possible causes for depressurizing of the process pipeline.

Investigation methods. Samples for investigations were prepared from templates cut out of a defective section of the pipe of process pipeline of 1020 mm diameter with 10 mm wall thickness.

Determination of chemical composition of metal of the fragments was conducted in X-ray fluorescent

Table 1. Chemical composition of X12CrMo5 steel, wt.%

Sample	C	Si	Mn	S	P	Cr	Ni	Cu	Mo	Ti
Outer side	0.13	0.27	0.48	0.008	0.020	4.6	0.30	0.13	0.55	<0.01
Inner side	0.13	0.27	0.48	0.008	0.022	4.6	0.30	0.13	0.56	<0.01
EU Certificate data	0.117	0.27	0.46	0.001	0.008	4.76	0.27	0.20	0.59	0.0061N
15KhM GOST 200072–74	0.15	<0.5	<0.5	<0.025	<0.03	4.5–6.0	<0.6	<0.2	0.45–0.60	<0.03

M.D. Rabkina — https://orcid.org/0000-0003-3498-0716, V.A. Kostin — https://orcid.org/0000-0002-2677-4667,
T.G. Solomiichuk — https://orcid.org/0000-0002-3038-8291

spectrometer CEP-01 «Elvax Light» and carbon analyzer GOU-1. Results of spectral analysis of pipe areas are given in Table 1, which shows the content of the chemical element in the selected sample.

For metallographic studies the microsections were polished with diamond pastes of different dispersity. The microstructure was detected by chemical etching of the microsections in 4 % solution of nitric acid. Analysis of the type of microstructures, as well as their photographing, was performed in NEOPHOT-32 microscope at different magnifications with application of digital photocamera OLYMPUS.

Obtained results and their discussion. Analysis of chemical composition of base metal (Table 1) showed that the pipe metal corresponds to steel of X12CrMo5 grade that reflects the chemical composition of metal of this steel manufactured by different foreign companies (Acroni, Bohler Welding Group, Tien Tai Electrode Co. Ltd., etc.). On the whole, analysis results are close, and correspond to the local analog of medium-chromium steel 15Kh5M.

Here, the somewhat lowered content of chromium and copper, as well as higher content of carbon in the metal, compared with the data of LAVIMONT BRNO Certificate should be noted. Presence of chromium in the solid solution determines formation of phase components, and also influences increase of strength properties, and metal susceptibility to brittle fracture, respectively. Note the considerable increase of sulphur and phosphorus, compared to the Certificate data. More over, based on EU Standard, sulphur content should not be higher than 0.005 %. Moreover, the Certificate does not specify the titanium content which is linked to nitrogen content, and which was detected in the presented fragments.

Metallographic analysis of the pipe base metal showed that its structure consists of ferrite matrix, alloyed by chromium and molybdenum, and dispersed carbides. Traces of general corrosion in the form of rust islands are observed both from the side of the pipe outer and inner surface. At intensive etching the carbide phase becomes more noticeable. In addition, in the middle sections along the sheet thickness, particularly in the longitudinal direction, the structural inhomogeneity of metal is clearly revealed in the form of alternating narrow dark and wider light bands, which is probably related to different content of carbon (Figure 2).

Macrostructure of welded joints is shown in Figure 3. The shape of the longitudinal weld looks like a cone. It is quite probable that prebending of the edges was not performed during pipe forming from a sheet. Considering that the longitudinal welds, having such a shape, are spaced around the ring at sequential joining

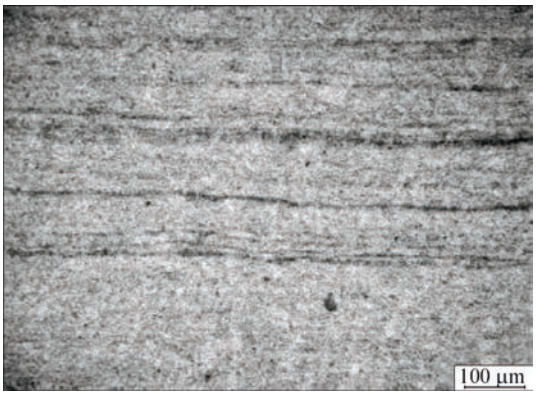

Figure 2. Base metal microstructure

of the shells by a site weld, additional welding stresses are known to develop because of violation of conjugation of the surfaces being welded. Circumferential site welds (Figure 3, *b*) also have certain defects. First, the height of the reinforcement bead, which should not be more than 2.5–4.0 mm, exceeds these values in a number of cases, similar to the longitudinal welded joint. Moreover, a lot of lacks-of-penetration and considerable contraction of the root layer are found.

It should be noted that at comparison of longitudinal welded joints made at the manufacturing plant and circumferential welded joints, made in site, rather high-quality performance of plant joints, compared with site butt joints, is found. However, analysis of welded joint microstructure allowed revealing the zones of lack-of-fusion also in the longitudinal weld. So, a defect was detected in the transverse microsection of the longitudinal welded joint, which is located on the boundary of the filling layer and by its shape repeats the contour of the bead in the weld pool (Figure 4). The defect area (in the plane, shown in the photo) reaches the size of 0.3×2 mm.

Despite the fact that the main problems in welding of high-strength steels are related to the fact that the welded joints are susceptible to cold cracking [4], this defect of the welded joint belongs to the category of defects of interbead lack-of-fusion. At the same time,

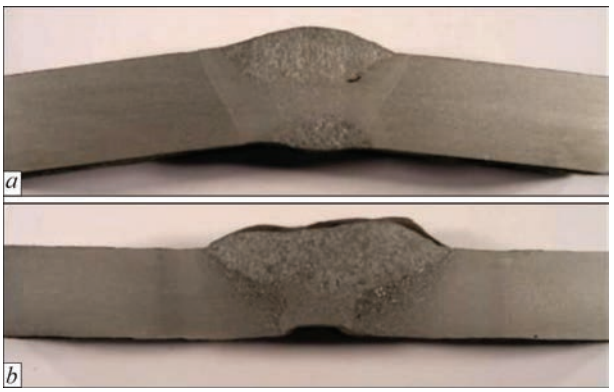

Figure 3. Macrostructure of welded joints: longitudinal (*a*) and circumferential (site) (*b*)

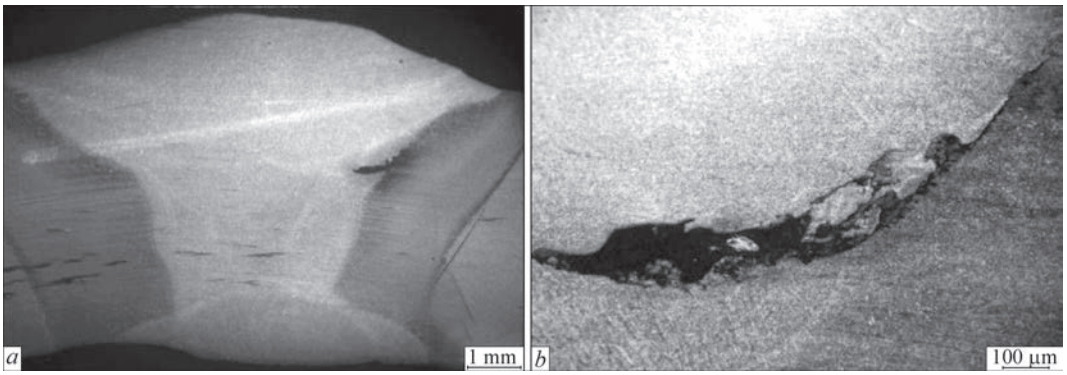

Figure 4. General view of the cross-section of the longitudinal welded joint (*a*) and interbead lack-of-fusion (*b*)

Figure 5. Delamination in the fracture of samples at tensile testing of longitudinal welded joints

similar defects are absent in the site welded joint in the part of the pipe, preserved after failure (Figure 3, *b*).

The microstructure of the circumferential weld metal is similar to that of the longitudinal weld, and also consists of a ferrite matrix, alloyed by chromium and molybdenum and finely-dispersed carbides.

Analysis of the results of mechanical testing showed that the metal of the studied pipe fragments has high strength characteristics at a sufficient level of ductility (Table 2). Here, the metal is practically isotropic in the sheet plane. However, as will be shown below, at tensile testing of welded joints no delamination was found in the sample neck (Figure 5) that is, most probably, due to anisotropy in Z-direction [5–7].

For evaluation of welded joint resistance to static and dynamic loads, the samples were cut out from both the longitudinal and circumferential welded joints (Table 3). As at tensile testing of welded joints fracture runs far from the deposited metal of the weld in all the cases, in the area of transition from the HAZ to the base metal, the mechanical characteristics (Table 3) represent the properties of the base (Table 2), rather than the deposited metal. Here, the yield limit, ultimate strength and relative elongation are 15–20 % higher in the longitudinal joints than in the circumferential ones.

Obtained results showed that unlike tensile testing (Table 3), at impact toughness testing of base metal the anisotropy phenomenon is manifested also in the

Table 2. Results of tensile testing of the base metal

Sample orientation	Yield limit σ_y, MPa	Ultimate strength σ_t, MPa	Relative elongation δ_5, %	Reduction in area ψ, %
Along the pipe axis	516.8–518.6	677.1–678.8	24.1–24.7	77.5–77.9
In the circumferential direction	515.1–516.8	674.3–676.4	24.8–25.3	73.3–77.5

Table 3. Results of tensile testing of welded joints

Welded joint	Yield limit σ_y, MPa	Ultimate strength σ_t, MPa	Relative elongation δ_5, %	Reduction in area ψ, %
Circumferential	451.5–485.5	590.4–629.6	18.9–19.7	72.0–75.1
Longitudinal*	520.1–560.9	667.0–672.5	23.5–24.0	73.0–73.1
*Delamination is observed in the rupture site.				

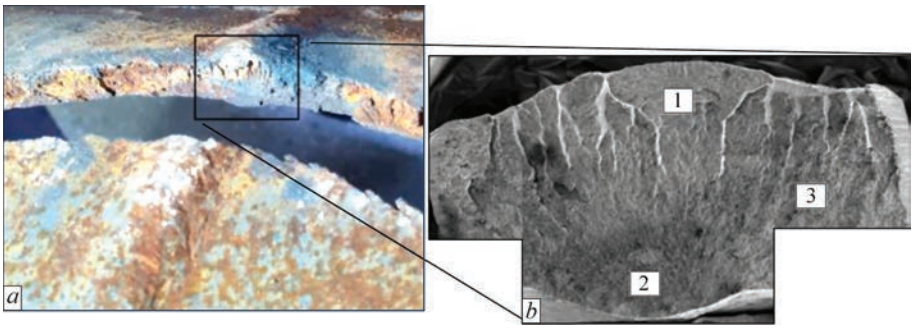

Figure 6. Appearance of a sample with the area of the start of pipe fracture in the longitudinal weld (*a*) and of the crack initiation region (*b*); *b* — ×10

rolling plane (Table 4). It leads, first of all, to different values of impact toughness along and across the rolling direction at room temperature, as well as to the spread of values at different testing temperatures [7].

Analysis of the influence of notch location on impact toughness values showed that at testing temperature of 20 °C at the notch location in the weld center, the impact toughness values of the longitudinal weld are 5 times higher than similar values of the circumferential weld, and at testing temperature of –10 °C they are more than 9 times (Table 4).

Note the inadmissibly low values of impact toughness of the site weld, particularly at minus temperature. So, for instance, in keeping with [8], the value of impact toughness in welded joints on samples with a sharp notch (*KCV*) in the weld center and on the fusion line at minimum service temperature should be not less than 29.4 J/cm^2 for pipes of 610–1020 mm diameter and 39.2 J/cm^2 for pipes of 1067–1420 mm diameter.

As the curvilinear shape of the fusion zone should be taken into account when making the notch in it, the spread of the results can be considered natural. However, in this case also the higher and more stable values of impact toughness of the longitudinal joint should be noted, as well as unstable values of impact toughness of the site joint, particularly at testing temperature of –10 °C (Table 4).

Thus, the performed laboratory studies that include determination of chemical and structural composition of the metal, allow stating that the pipe metal corresponds to the medium-chromium steel of X12CrMo5 grade. Here, it should be noted that mechanical testing revealed some indications of rolled stock anisotropy in the transition to the HAZ, which are manifested, primarily, in typical delamination of base metal that agrees with the concepts presented in work [5]. As regards the weld metal, extremely low and unstable values of impact toughness of site welded joints were established at impact bend testing, particularly, at minus temperature. At the same time, a defect in the form of interbead lack-of-fusion was revealed in the longitudinal weld. As will be shown below, this defect could exactly be one of the triggers, which led to fracture of the studied process pipeline.

Investigations of fracture surface. Visual-optical analysis of a fragment of broken pipe showed that the area of maximum opening of the crack is located in the region of the longitudinal weld crossing the HAZ of the circumferential weld (Figure 6). Here, it was found that the macroscopic features of the crack passing, namely the chevron pattern, change from one direction to the opposite one exactly in this region that was classified as the point of the start of pipe destruction.

Comparison of macro- and microstructure of the longitudinal welded joint (Figure 3, *a*; Figure 4) and morphology of fracture surface (Figure 6, *b*) allowed distinguishing three main areas in the destruction center: *1* — facing layer with filling layers; *2* — root layer; *3* — near-weed zone.

The facing layer is characterized by the dendritic structure in the fracture (Figure 6, *b*) that formed during liquid metal solidification in welding. Along-

Table 4. Results of impact bend testing of Charpy samples (*KCV*)

Number	Area of sample cutting out	Point of making the notch	*KCV*, J/cm^2	
			–10 °C	20 °C
1	Circumferential weld	Fusion zone	15.0–60.0	22.9–32.4
		Weld center	8.3	25.9–29.4
2	Longitudinal weld	Fusion zone	29.3–50.8	59.1–95.2
		Weld center	36.0–78.6	157.6–157.7
3	BM in the longitudinal direction	–	34.2–54.5	139.5–149.1
4	BM in the circumferential direction	–	32.7–34.5	159.7–280.2
Note. Notch through pipe wall thickness.				

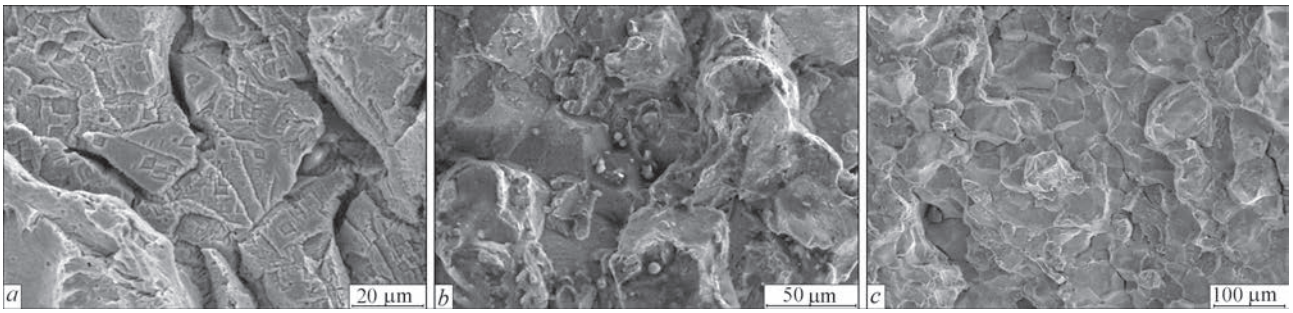

Figure 7. Fracture mode: *a* — facing weld; *b* — root weld; *c* — near-weld zone

side fracture in the primary dendritic structure, also cleavage facets and twins, characteristic of the secondary structure, are observed in the fracture [9]. In both the cases, formation of secondary cracks is in place (Figure 7, *a*, *b*), which cross the fracture surface. Presence of a viscous component in the fracture in the form of river pattern should be also noted. Appearance of secondary cracks, combined with tough regions against the background of overall brittleness is indicative of instability of crack propagation.

Analysis of fracture in the root layer showed that fracture occurred on the boundaries of secondary grains and has a stone-like nature (Figure 7, *b*). This region turned out to be strongly oxidized. Appearance of corrosion products is obviously related to the results of diffusion penetration of active elements (oxygen, hydrogen, carbon) into the root weld from the inner surface of the pipe in operation.

The fracture surface in the near-weld zone (Figure 7, *c*) is also characterized by stone-like fracture with enrichment by sulphur and phosphorus between the grains.

Thus, considering the possibility of appearance of underbead defects in the longitudinal welded joint (Figure 3, *a*; Figure 4), it is possible that such lacks-of-fusion or solidification microcracks could provoke initiation of brittle cracks at the initial stage of destruction. Their further propagation was, probably, promoted by a number of other reasons, for instance, presence of residual welding stresses due to violation of postweld heat treatment; failure to follow the pressing mode; poor design of pipeline fitting, etc. Here, the macrocrack propagated from the destruction center to both sides around the pipe ring which indicates that the axial stresses in the pipe under the impact of internal pressure are much higher then the hoop stresses. This assumption requires further study.

Conclusions

1. It is determined that the base metal of the broken pipe fragment belongs to medium-chromium steel by its composition that corresponds to local analog 15Kh5M, with a typical microstructure, consisting of equiaxed ferrite base, alloyed by chromium and molybdenum and dispersed carbides.

2. It is shown that crack propagation from the start of its initiation to both sides around the ring occurs in the brittle mode that is indicative of a typical chevron-type pattern of the fracture surface, which can be related to presence of high residual stresses, most probably due to violation of their relieving technology.

3. It is found that the start of fracture is located in the point of the longitudinal weld crossing the HAZ of the circumferential (site) weld, and it was triggered by defects in welds, in particular, interbead lacks-of-fusion. Here, exceeding the normative values of the reinforcement bead height was detected, which is inherent to both kinds of joints. More over, a lot of lacks-of-penetration are found that is, largely, characteristic for a site circumferential weld.

1. *Girgin* Serkan, K. (2015) *Elisabeth Lessons Learned from Oil Pipeline Natech Accidents and Recommendations for Natech Scenario Development – Final Report.* ©EU. Abstract, Published.
2. Kushnareva, O.V., Golubaev, D.V. (2018) Analysis of accident causes on objects of main gas-and-oil pipelines*:* Problems and solutions. *Master's J.*, **1**, 37–43.
3. Kuznetsova, N.V., Krasnokutsky, A.N. (2012) Experience of calculation and design of transfer pipelines. *Tekhnologii Nefti i Gaza*, **3**, 54–59 [in Russian].
4. Lobanov, L.M., Poznyakov, V.D., Makhnenko, O.V. (2013) Formation of cold cracks in welded joints from high-strength steels with 350-850 MPa yield strength. *The Paton Welding J.*, **7**, 8–13.
5. Lobanov, L.M., Girenko, V.S., Rabkina, M.D. (2001) Anisotropy of crack resistance characteristics as one of the causes of crack initiation in welded bridge spans. In: *Diagnostics, life and reconstruction of bridges and building structures*, Transact., Lviv, Kamenyar, Issue 3, 138–147 [in Russian].
6. Farber, V.M., Khotinov, V.A., Belikov, S.V. et al. (2016) Separations in steels subjected to controlled rolling, followed by accelerated cooling. *Physics of Metals and Metallography*, 117, 407–421.
7. Usov, V.V., Girenko, V.S., Rabkina, M.D. et al. (1993) Influence of crystallographic texture on anisotropy of fracture characteristics of low-alloyed steel of controlled rolling. *Fizikokhimicheskaya Mekhanika Materialov,* **2**, 47–52 [in Russian].
8. *TU 1381-003-47966425–2006: Steel longitudinal welded pipes with an outer diameter of 610–1420 mm* [in Russian].
9. Fellous, J. (1982) *Fractography and atlas of fractograms.* Moscow, Metallurgiya [in Russian].

Received 01.02.2021